

# Is there an ideal insertion angle and position for orthodontic mini-implants in the anterior palate? A CBCT study in humans

Kathrin Becker,<sup>a</sup> Justine Unland,<sup>a</sup> Benedict Wilmes,<sup>a</sup> Nour Eldin Tarraf,<sup>b</sup> and Dieter Drescher<sup>a</sup>  
Düsseldorf, Germany, and Sydney, Australia

**Introduction:** Orthodontic mini-implants are frequently used to provide additional anchorage for orthodontic appliances. The anterior palate is frequently used owing to sufficient bone quality and low risk of iatrogenic trauma to adjacent anatomical structures. Even though the success rates in this site are high, failure of an implant will result in anchorage loss. Therefore, implants should be placed in areas with sufficient bone quality. The aim of the present study was to identify an optimal insertion angle and position for orthodontic mini-implants in the anterior palate. **Methods:** Maxillary cone-beam computed tomographic (CBCT) scans from 30 patients (8 male, 22 female, age  $18.6 \pm 12.0$  years) were analyzed. To assess the maximum possible length of an implant, a 25-reference-point grid was defined: 5 sagittal slices were extracted along the median plane and bilaterally at 3 mm and 6 mm distances, respectively. Within each slice, 5 dental reference points were projected to the palatal curvature at the contact point between the cuspid (C) and first bicuspid (PM1), midpoint of PM1, between PM1 and PM2, midpoint of PM2, and between PM2 and the first molar (M1). Measurements were conducted at  $-30^\circ$ ,  $-20^\circ$ ,  $-10^\circ$ ,  $0^\circ$ ,  $10^\circ$ ,  $20^\circ$ , and  $30^\circ$  to a vector placed perpendicular to the local palatal curvature. Statistical analysis was conducted with the use of R using a random-effects mixed linear model and a Tukey post hoc test with Holm correction. **Results:** High interindividual variability was detected. Maximum effective bone heights were detected within a T-shaped area at the midpoint of PM1 and contact point PM1-PM2 ( $P < 0.01$ ). Within the anterior region a posterior tipping was advantageous, whereas in the posterior regions an anterior tipping was beneficial ( $P < 0.01$ ). In the middle of the median plane, tipping did not reveal a significant influence. No gender- or age-related differences were observed. **Conclusions:** Within the limitations of this study, optimal insertion positions were found within a T-shaped area at the height of PM1-PM2 in the anterior palate. In general, a posterior tipping was beneficial at anterior positions, and an anterior tipping appeared beneficial at posterior positions. High interindividual variation was found and should be carefully considered by the clinician. (Am J Orthod Dentofacial Orthop 2019;156:345-54)

Orthodontic treatment with the use of fixed appliances requires sufficient anchorage. In the past decade, orthodontic mini-implants have become popular because they provide additional skeletal anchorage and increase the overall treatment spectrum.

<sup>a</sup>Department for Orthodontics, University Hospital Düsseldorf, Düsseldorf, Germany.

<sup>b</sup>Private practice, Sydney, Australia.

Kathrin Becker and Justine Unland are joint first authors and contributed equally to this work.

All authors have completed and submitted the ICMJE Form for Disclosure of Potential Conflicts of Interest, and none were reported.

Address correspondence to: Kathrin Becker, Department for Orthodontics, University Hospital Düsseldorf, D-40225 Düsseldorf, Germany; e-mail, [kathrin.becker@med.uni-dueseldorf.de](mailto:kathrin.becker@med.uni-dueseldorf.de).

Submitted, July 2018; revised and accepted, September 2018.

0889-5406/\$36.00

© 2019 by the American Association of Orthodontists. All rights reserved.

<https://doi.org/10.1016/j.ajodo.2018.09.019>

Several studies have demonstrated their efficacy for en masse retraction, Class III therapy, space closure, and many other applications<sup>1-4</sup> for both adults and children.<sup>5</sup> The anterior palate has become a favored insertion site owing to the ability to place implants with larger dimensions, thus offering greater stability.<sup>6,7</sup> Despite the advantages and frequent use, there are risks and complications associated with the insertion of mini-implants, such as trauma to dental roots, nerve involvement, perforation into the nasal or maxillary sinus, and anchorage loss.<sup>8</sup> The latter may occur when implants become loose owing to insufficient bone quality or inflammation.<sup>9</sup>

Because sufficient bone quality in the anterior palate is crucial to obtain appropriate implant stability, it has been evaluated in several studies.<sup>9-24</sup> Several reports

suggest that bone quality is superior within a T-shaped zone encompassing the anterior palate and the median suture.<sup>25-27</sup>

At this stage there are contradictory reports on the suitability of the median suture posterior to the second rugae. Pronounced interindividual variances have been reported,<sup>28</sup> and one study with a very large sample size reported on bone height decreases posterior to the second rugae.<sup>20</sup> In addition, most studies evaluated bone height perpendicular to the occlusal plane, which is in contrast to the clinical recommendation to place the mini-implants perpendicular to the palatal curvature, making measurements perpendicular to the occlusal plane of limited relevance for the clinician. The ideal insertion angle at different positions in the palate may be more clinically relevant.

The aim of the present investigation was to measure bone thicknesses perpendicular to the palatal curvature with angles varying from  $-30^\circ$  to  $+30^\circ$  at different positions within CBCT images, and to classify potential locations based on their suitability for orthodontic mini-implants. As a second aim, sex- and age-related differences were evaluated.

## MATERIAL AND METHODS

This cross-sectional study included a total of 30 patients (22 female subjects, mean age  $20.1 \pm 13.1$  years; and 8 male subjects, mean age  $13.5 \pm 5.0$  years). All patients had been treated at the Department for Orthodontics, Universitätsklinikum, Düsseldorf, Germany).

The inclusion criterion was that a cone-beam computed tomographic (CBCT) scan was obtained in the years 2010–2014 with the use of the Pax-Duo 3D (Orange Dental, Biberach, Germany) at 90 kV, 3.0–5.5 mA, 24 s exposure time, and 0.2 mm isotropic resolution.

The exclusion criteria were syndromes or craniofacial malformations, pathologic processes in the maxilla, missing teeth in the maxilla, and palatally displaced teeth.

The study protocol was approved by the local Ethical Committee (IRB number 5418). No informed consent was required, because all CBCT images had been obtained in the past, they were clinically justified, and the data were anonymized before the investigation.

Alignment of the CBCT scans according to the occlusal plane and the median-sagittal plane was performed with the use of Osirix for Mac OS (version 5.8.2, 32 bit; Pixmeo Bernex, Switzerland). Measurement positions were constructed by means of the following steps. (1) Extraction of sagittal slices along the midpalatal suture, 3 mm lateral and 6 mm lateral,

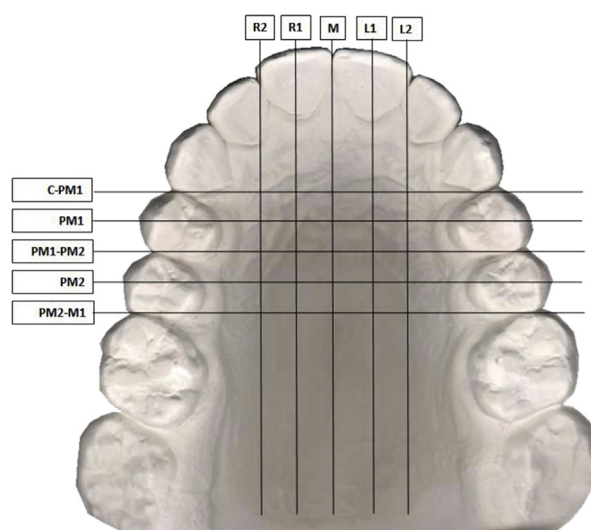


**Fig 1.** Visualization of the measuring grid (occlusal view): Effective bone height and BV/TV were measured at 25 measuring points at different angulations. For each sagittal view, the respective slices were extracted from the volumetric CBCT data sets, ie, R2/L2 (left and right 6 mm paramedian slices), R1/L1 (right and left 3 mm paramedian slices), and M (median slice). Measurements were performed at the interproximal contact of canine and first bicuspid (C-PM1), first bicuspid (PM1), interproximal contact of the 2 bicuspids (PM1-PM2), second bicuspid (PM2), and interproximal contact to the first molar (PM2-M1).

were extracted. (2) Transversal reference lines were constructed perpendicular to the midpalatal suture. These reference lines were located in such a way that they passed through the contact points between the canines and the first premolars (C-PM1), between the first and the second premolars (PM1-PM2,) and between the second premolar and the first molar (PM2-M1). Thus, they enabled projection of the dental landmarks to the measurement grid. (3) Additional reference lines (dental projections) were constructed at the central aspect of the 2 bicuspids, ie, PM1 and PM2. These reference points were constructed by computing the midpoint of the vector from C-PM1 to PM1-PM2 and the midpoint of the vector from PM1-PM2 to PM2-M1. (4) A measuring grid consisting of 25 measuring points (intersections of sagittal and transverse reference lines) was generated (Fig 1). All measurements were performed within the 5 sagittal slices at the respective dental projections after export of the respective slices.

All morphometric measurements were performed with the use of the ImageJ software program (version 2.0.0-rc-39/1.50 b; National Institutes of Health, US)

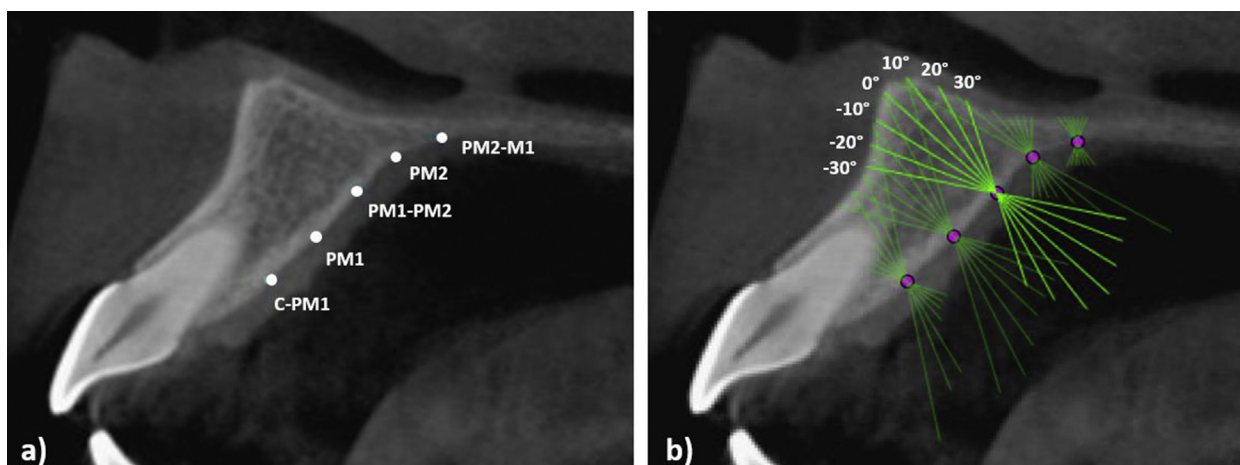


**Fig 2.** Examples for sagittal slices extracted from CBCT to perform effective bone height and bone fraction (BV/TV) measurements at different angulations: **a**, Projections of the measurement points (C-PM1, PM1, PM1-PM2, PM2, and PM2-M1) to the palatal bone plate at a paramedian slice. **b**, Measurement of effective bone height (and BV/TV) was performed at 7 different angulations ( $-30^{\circ}$  to  $30^{\circ}$ ).  $0^{\circ}$  is equivalent to a perpendicular insertion.

for Mac OS. All reference points were identified at each slice (Fig 2, a) and a tangent was matched to the bony margin of each reference point. All measurements (see below) were performed perpendicular ( $0^{\circ}$ ) to the tangent and subsequently with an angulation of  $-30^{\circ}$ ,  $-20^{\circ}$ ,  $-10^{\circ}$ ,  $10^{\circ}$ ,  $20^{\circ}$  and  $30^{\circ}$  (Fig 2, b).

Effective bone heights were measured between the cortical margins from the palate and the nasal or maxillary sinus with the use of the measurement line tool in ImageJ. If the measurement line intersected with tooth roots or the incisive canal, the measurement was stopped at the respective anatomic positions.

Bone fraction (BV/TV), defined as the relative amount of calcified bone (%) within a region of interest (ROI; 5 mm thickness), was obtained with the use of the volume fraction tool in the ImageJ plugin BoneJ. A subset of 22 CBCTs were found eligible for this analyses, whereas the remaining scans had to be excluded because of artefacts from mini-implants located in the anterior palate.

Because CBCT is usually not calibrated, ie, gray values do not exactly correspond with the respective Hounsfield units, a histogram normalization was required. To achieve normalization, the respective minimum (air) and maximum (enamel) gray values were measured in each sagittal slice (Fig 3, a) and set as minimum and maximum gray values.

To segment bone tissue, the lower threshold level was set to 33% (Fig 3, b), because this value provided the most consistent segmentation. BV/TV was measured at each reference point along the respective measurement

line and the above-mentioned angulations with the use of a thickness of 5 mm (Fig 3, c). If the ROI was not entirely surrounded by bone, eg, because of intersection with the nasal cavity, it was cranially shortened until it contained bone tissue only.

After assessment of effective bone height at different insertion angles and the respective BV/TV values, the data were pooled by insertion position and classified as follows: green (high suitability): effective bone height  $>6.5$  mm, BV/TV  $>0.4$  mm, no intersection of the measurement line with tooth roots or incisal canal; yellow (moderate suitability): effective bone height 5.0-6.5 mm, no intersection of the measurement line with tooth roots or incisal canal; or red (low suitability): effective bone height  $<5.0$  mm or intersection with tooth root or incisive canal.

In all locations classified as “green” or “yellow,” best insertion angles were identified by comparison of locally available effective bone heights.

### Statistical analysis

The statistical analysis was performed with the use of R.<sup>29</sup> For descriptive purposes, data were summarized with the use of boxplots. Because data were partially dependent (multiple measurements per patient), a linear mixed effects (LMER) model was used for statistical comparison (random effect: patient; fixed effects: age and sex, or angle, sagittal position, and transversal position). To assess if qualitative differences existed between the mixed model against a model without the factors in

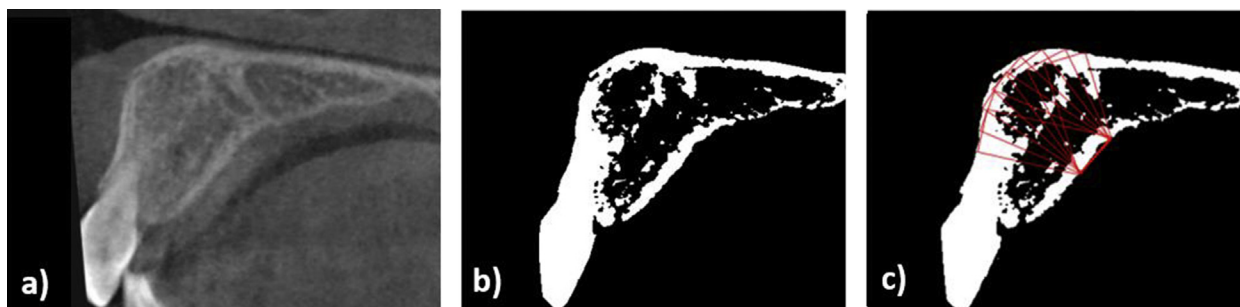


**Fig 3.** Measurement of bone fraction (BV/TV), **a**, Sagittal slices were used to evaluate BV/TV values. **b**, Bone segmentation was performed after calibration according to the individual minimum (air) and maximum (enamel) gray values of the respective slice and a threshold level of 84 in the 8 bit image. **c**, Example for BV/TV evaluation at PM1-PM2 for each angulations ( $-30^{\circ}$  to  $30^{\circ}$ ) within a region of interest of 5 mm thickness around the measurement line (not shown). The values were exported as percentages.

question, analysis of variance (ANOVA) was conducted. Post hoc comparisons were performed with the use of Tukey multiple comparison test and the Holm  $P$  value correction method.

The suitabilities of different measurement positions were classified based on the findings from the mixed model and the proximity to tooth roots and the incisal canal. Finally, the local impact of the insertion angle at each reference point was assessed by computing the linear mixed effects model for 1 random effect (insertion angle) and 1 fixed effect (patient). This model was compared against a model without this factor by means of ANOVA. The results were assumed to be significant at  $P < 0.05$ .

## RESULTS

The association between effective bone height and patient age and sex was tested by means of ANOVA comparing an LMER with the effects of interest (fixed effects: age and sex; random effect: patient) against a model without these effects (random effect: patient only). This analysis revealed no significance ( $P = 0.81$ ), meaning that age and sex could not explain the differences of bone thicknesses.

Descriptive analyses showed distinct variability of available effective bone height at different insertion points and angles. Paramedian effective bone heights were generally higher than median positions, increasing from C-PM1 to PM1. They remained higher for posterior insertion angles at PM1-PM2 and decreased toward PM2 and PM2-M1. PM1 revealed the greatest effective bone height at paramedian positions of  $8.38 \pm 3.75$  mm (3 mm paramedian) and  $8.42 \pm 3.70$  mm (6 mm paramedian),

whereas the greatest effective bone height at median positions was found at PM1-PM2 ( $6.35 \pm 3.09$  mm; Fig 4).

BV/TV decreased from anterior to posterior positions and had similar values in median and paramedian positions. Adjacent to the incisal canal, BV/TV was negligible (Fig 5).

The ANOVA revealed significance for the LMER with the factors sagittal position, transversal position, and insertion angle ( $P < 0.001$ ). These factors remained significant when the model was reduced to single factors only ( $P < 0.01$ ). This means that both the insertion positions and respective angles could explain the differences of the effective bone heights. The post hoc multiple comparison test yielded significant differences between all sagittal insertion points ( $P < 0.01$ ), and between median and lateral points at 3 mm, as well as between median and lateral points at 6 mm ( $P < 0.001$ ). However, no significant differences were identified between lateral points at 3 and 6 mm ( $P = 0.25$  to  $P = 1.0$ ).

For each location in the measurement grid, the optimal local insertion angles (when available) were computed by means of ANOVA and Tukey post hoc multiple comparison test (Supplementary Table, available at [www.ajodo.org](http://www.ajodo.org)). Significant differences in effective bone height for different angulations were detected for all paramedian and median C-PM1 positions. In these positions, a posterior inclination was most beneficial. A posterior angulation was also most beneficial at the median and paramedian PM1 (6 mm lateral, right site only).

The greatest effective bone height was found for an anterior angulation at the paramedian PM1-PM2 and PM2-M1 points and at all PM2 points.

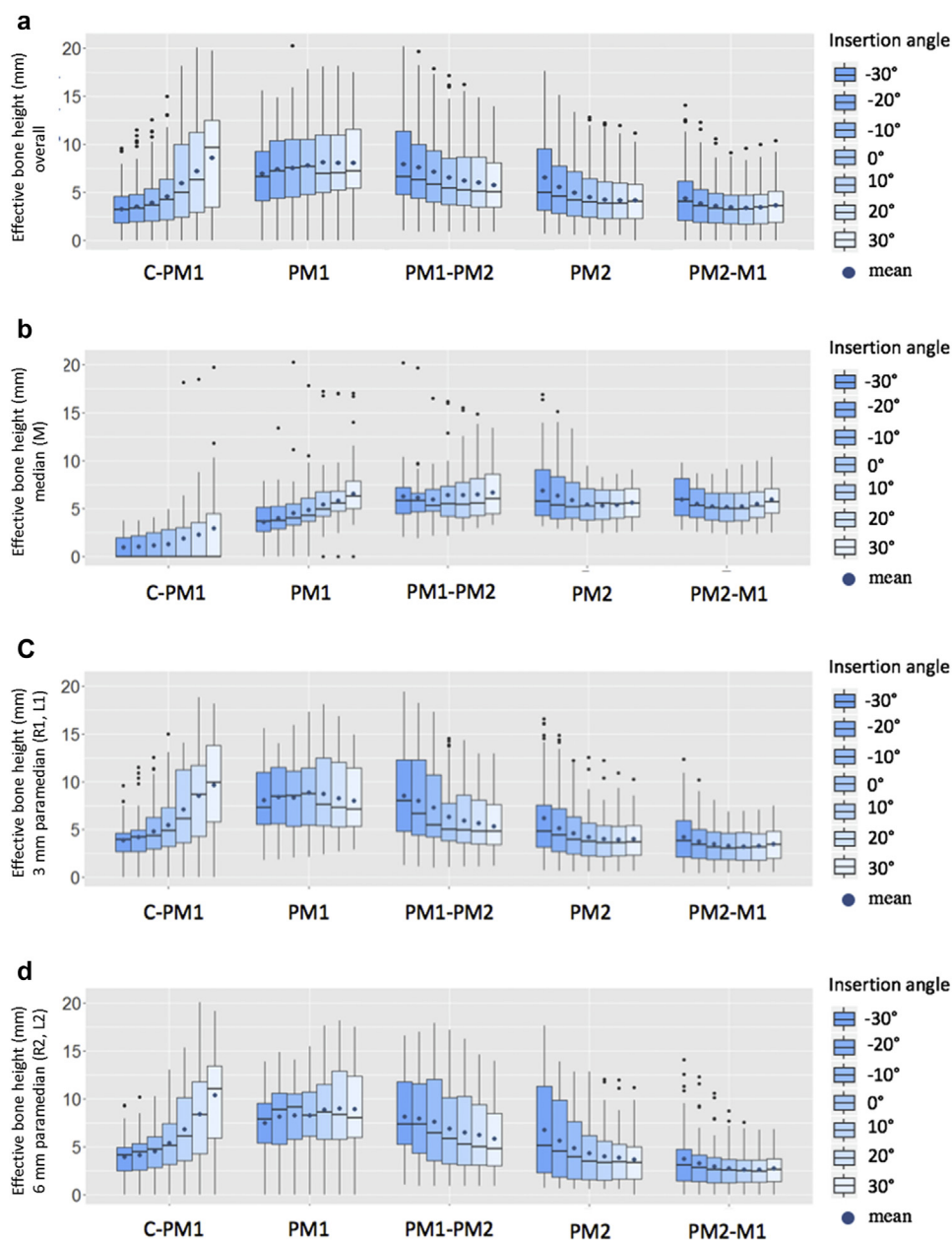


**Fig 4.** Boxplots showing the medians and interquartile ranges for effective bone height measurements **(a)** overall (pooled values) and at **(b)** median (M), **(c)** 3 mm paramedian (pooled R1 and L1 values), and **(d)** 6 mm paramedian (pooled R2 and L2 values).

The ANOVA revealed significance for the LMER with the factors sagittal position, transversal position, and insertion angle ( $P < 0.001$ ) and remained significant when reducing the model to 1 factor only ( $P < 0.001$ ). The post hoc multiple comparison test yielded significant differences between the median plane (M) against all of the paramedian planes (R2, R1, L1, L2;  $P < 0.001$ ) as well as between L2 toward

L1 and between L2 toward R1 ( $P < 0.01$ ). Furthermore, there was a significant difference in bone fraction at the insertion points PM2 and PM2-M1 against every other sagittal insertion points ( $P < 0.001$ ). At these points, BV/TV was lower compared with the remaining positions.

The insertion points and their classification are shown in [Figure 6](#). All PM1-PM2 insertion points and

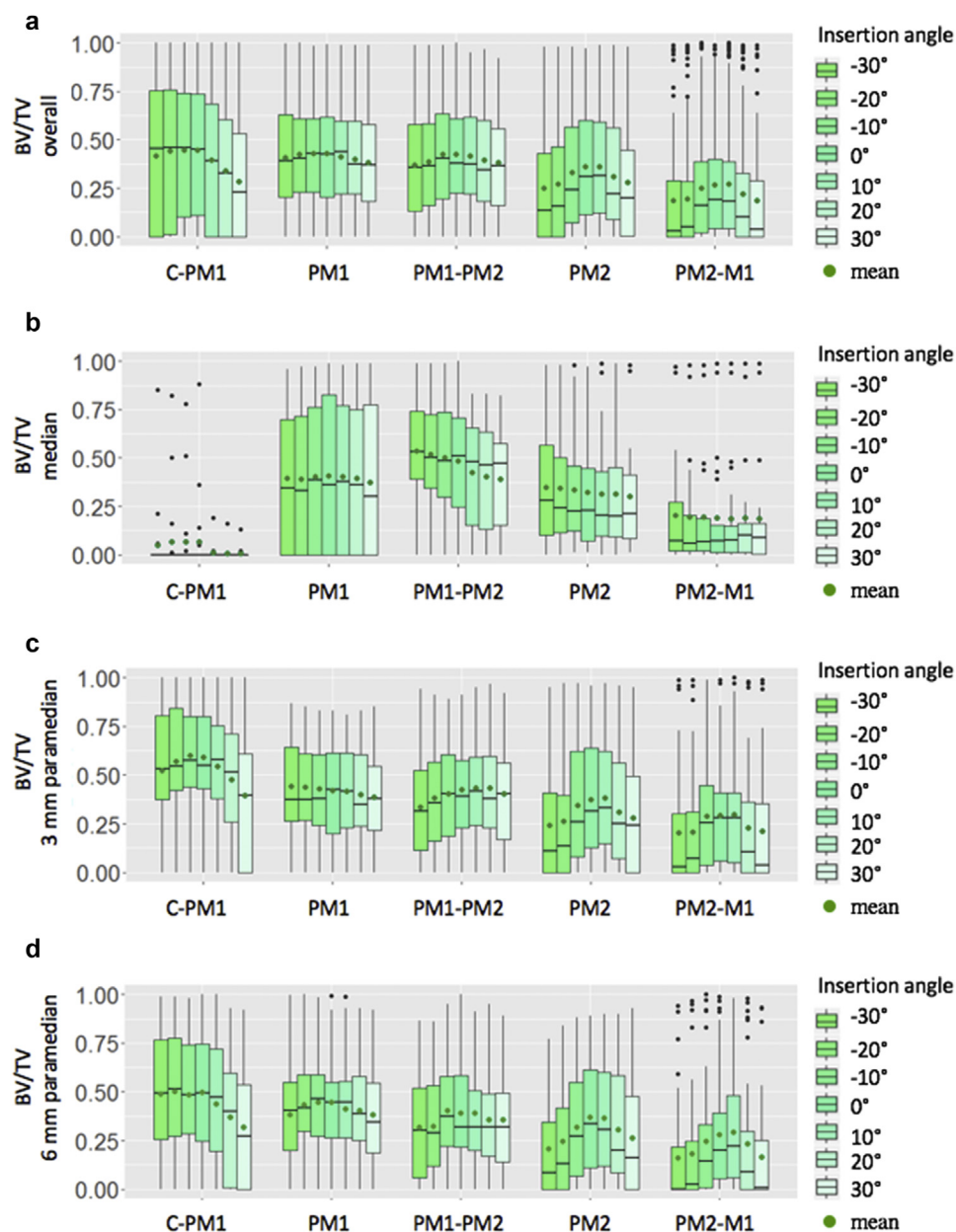


**Fig 5.** Boxplots showing the bone fraction values (BV/TV) (a) overall (pooled values) and at (b) median, (c) 3 mm paramedian, and (d) 6 mm paramedian.

all paramedian PM1 insertion points were classified as “green.” The median insertion points PM1, PM2, and PM2-M1 were classified as “yellow.” The L1/L2 and R1/R2 paramedian insertion points PM2 and PM2-M1 were classified as “red” owing to a low mean effective bone height. The anterior C-PM1 insertion points were classified as not suitable due to risk of damage of the anterior tooth roots and incisal canal. The optimal

insertion angle (maximum effective bone height) is included in Figure 6 for all points classified as “green” or “yellow.”

## DISCUSSION

This study aimed to assess if specific insertion angles are beneficial for orthodontic mini-implants in the anterior palate. The overall potential benefit of a specific

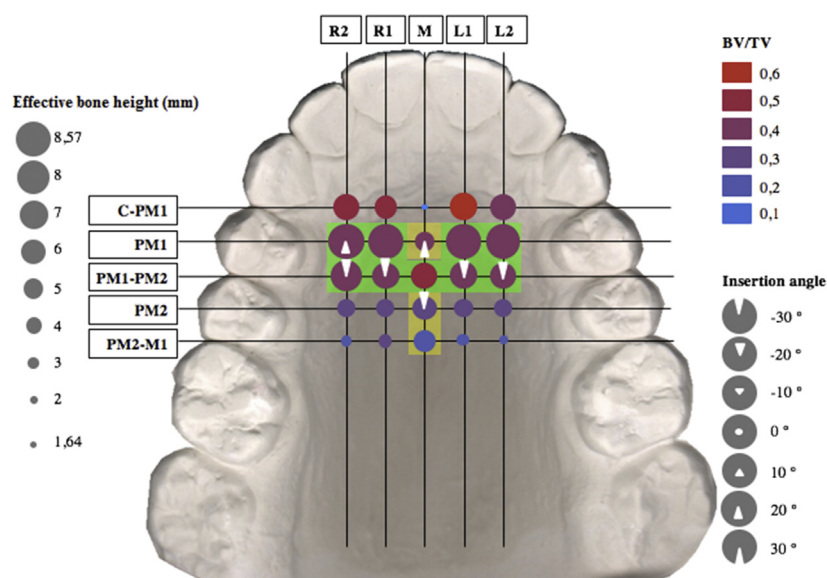


**Fig 6.** Orientation map of the anterior palate summarizing the effective bone height and bone fraction measurements from all patients at the respective positions. For each point, effective bone height and bone fraction values obtained at different angles were pooled and encoded by the point diameter or color, respectively. The insertion angle offering the greatest effective bone height at each point is indicated by white triangles. The eligibility of potential mini-implant insertion areas was classified as follows: *green* = ideal (effective bone height >6.5 mm and BV/TV > 0.4); and *yellow* = limited (effective bone height 5.0-6.5 mm). The paramedian C-PM1 values were not classified as ideal or limited owing to high variability among patients and thus high risk of root damage.

angle was tested as well as for specific common paramedian and median locations. Potential locations and angles were then classified based on the quantity of bone support for orthodontic mini-implants. As a secondary outcome, sex- and age-related differences were evaluated.

To evaluate which insertion angle would be most beneficial, differences in effective bone height and densities at different sagittal and transversal locations were evaluated. Our analysis confirmed previous findings of greatest bone thicknesses and bone fraction values between the first and second premolars at the palatal suture and a decrease of effective bone height in a posterior direction.<sup>20,21</sup> Effective bone heights reached maximum values slightly anterior and lateral to the first premolars at both the 3 mm and the 6 mm paramedian positions, whereas height and bone fraction values decreased at both paramedian positions more posteriorly. This is similar to previous findings.<sup>17,30</sup>

At positions anterior to the first premolar, the risk of touching to nasopalatine nerve was highest, which is in agreement with another recent investigation.<sup>31</sup>

A significant impact of the insertion angle on primary stability of mini-implants has been reported previously.<sup>32</sup> In addition, this investigation shows that the

insertion angle also affects the available effective bone height for implant insertion. However, our analyses revealed that the insertion angle is relevant only at specific positions, namely, at the most posterior and anterior median positions but not at the region of highest median bone availability.

For paramedian insertion lateral to the second premolar and contact point PM1-PM2, the insertion angle also proved to be significant, whereas bone thickness was in general too low for placements more posteriorly. For median and paramedian placement, 30° to 20° tipping of the implant to the posterior proved to be most effective at the anterior positions. In contrast, anterior tipping of -30° yielded the best bone support at the posterior median and paramedian positions (Fig 6).

As a secondary outcome, age- and sex-related differences in effective bone height and bone fraction were evaluated. Conflicting findings have been reported in the literature regarding differences in bone quality or height with respect to age,<sup>10,11,15,21,33-35</sup> in agreement with our present study. This finding could be explained by the fact that subjects included in the previous studies were rather young ( $18.6 \pm 12$  years on average in our study). From an osteologic

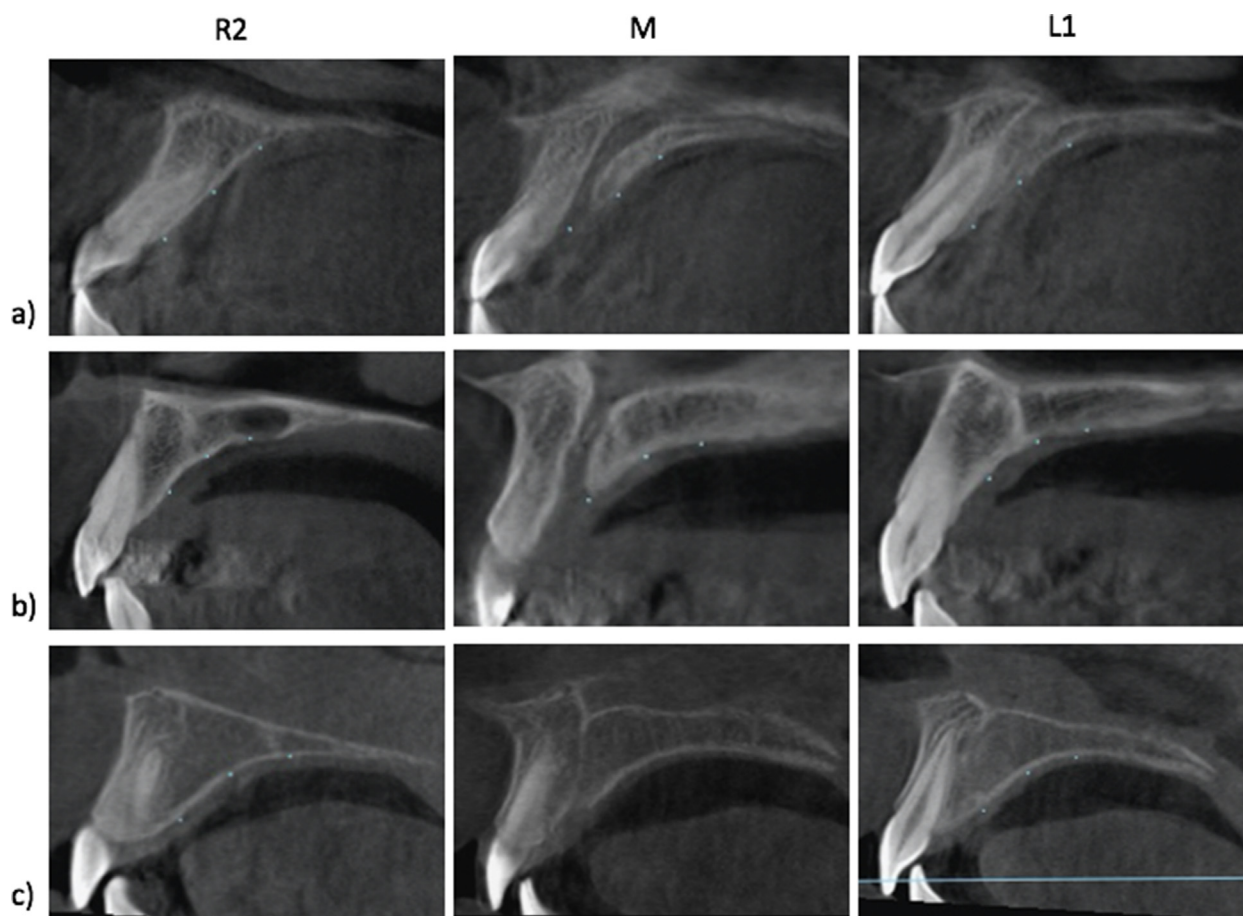


**Fig 7.** CBCT slices of patients showing examples for minimal, median, and maximum effective bone height values in the right 6 mm paramedian (R2), median (M), and left 3 mm paramedian (L1) slices. **a**, Patient with least effective bone height values (female, 15 y): effective bone height of 0 mm at C-PM1 (R2), PM1 (R2), and at C-PM1 (M). **b**, Patient with median effective bone height values (female, 39 y): effective bone height of 13 mm at PM1-PM2 (R2), 7 mm at PM1, PM1-PM2, PM2, and PM2-M1 (M), and 13 mm at PM1-PM2 (L1). However, effective bone height decreased to 0 mm at R2 at PM2-M1 and at C-PM1 (M). Effective bone height still amounted to 7 mm for anterior angulations at PM1-PM2 (L1). **c**, Patient with greatest effective bone height values (male, 13 y): effective bone height of 20 mm at PM1 (M) and 18 mm at C-PM1 (R2) and PM1 (L1).

perspective, peak bone mass occurs in the late twenties or early thirties,<sup>36</sup> so age-dependent changes may only be observed if a greater age range is examined.

Controversial findings have also been reported on association between sex and effective bone height. Whereas significant associations were found in a few studies,<sup>15,17,33</sup> no significant differences were identified in studies by Gracco et al,<sup>21</sup> Ryu et al,<sup>10</sup> Stockmann et al,<sup>37</sup> and Sumer et al,<sup>34</sup> also in agreement with the present investigation. However, the conflicting findings may be explained by subject age, because studies comparing bone samples from patients of different ages reported significant sex-dependent differences for postmenopausal women compared with older men.<sup>38,39</sup>

Different methods to assess palatal effective bone height have been reported in the literature. Two-dimensional measurements with the use of lateral cephalograms are of limited relevance owing to superimposition of anatomic structures. Bone height morphometry results can vary significantly between values obtained from lateral cephalograms and volumetric images.<sup>40</sup> Therefore, analysis of CBCT images is a common practice to evaluate bone availability in the anterior palate.<sup>31,33,34</sup> Insertion angles and effective bone height have been evaluated with respect to different reference planes, of which the sagittal and coronal planes from CBCT have been used in most cases.<sup>31,40</sup> In contrast, we aligned all of the data sets to the occlusal plane

before analysis to allow consistent alignment of the CBCT images for comparison. The slices were extracted either at the median or the paramedian plane. Because implant placement is recommended to be performed perpendicular to the palatal surface, we considered effective bone height in this direction to be most relevant for the clinician. Therefore, implant placement perpendicular to the palatal surface was defined as the default 0° position, and bone support after tipping the implant from -30° to the anterior to +30° to the posterior was also evaluated.

Bone fraction measurements on CBCT images have been described as problematic due to the huge variance of gray values and missing or inaccurate Hounsfield units in CBCT.<sup>41,42</sup> In the present investigation, before the determination of the bone fraction, each sagittal slice was normalized by setting air to 0 and the enamel to 255. By this approach, the bony structures could be accurately identified independently from their actual gray value in the respective slice. To provide consistent calibration and comparability, all images were obtained with the use of the same CBCT machine.

Variability of effective bone height between individuals was very high (Fig 7), in agreement with previous studies.<sup>9,13,17,23</sup> Given the high variability of the amount of bone in the investigated regions, the question arises whether results are reliable enough to justify general recommendations for palatal implant insertion sites and angles. Some authors support this notion,<sup>14,21,37</sup> whereas a systematic review of literature concluded that bone availability may be too low in some cases to achieve sufficient implant stability for maximum anchorage and that individual assessment is required.<sup>43</sup> Varying bone qualities were also observed in autopsy material from 22 subjects, but the majority of samples provided sufficient bone for temporary skeletal anchorage.<sup>35,44</sup> However, the present study confirmed that individuals with a very low effective bone height of <2 mm do exist, and it is likely that these individuals would be prone to implant failure. Whether identification of these subjects is possible from lateral cephalograms or the type of clinically visible palatal curvature needs to be evaluated in future studies.

Limitations of this study were that only sagittal tipping of the implant was investigated whereas lateral tipping may also be relevant in median as well as paramedian positions. Figure 6 illustrates the investigated insertion positions and angles as a map. However, only the insertion angle providing maximum bone support was selected instead of all angles that revealed significance. The impact of tipping of the implant was tested for maximum bone support only, even though bone fraction also affects implant stability. Bone fraction

was tested only at the specific locations, because we considered that the clinician will first look for maximum bone and then check the bone fraction at the specific locations.

## CONCLUSIONS

This investigation supports the assumption of a T-shaped area located in the anterior palate providing superior bony support for orthodontic mini-implants.<sup>26,27</sup> However, this region may be slightly narrower and smaller than previously suggested. Optimal bone support existed only lateral to the first premolar for paramedian and extended to the second premolar for median placements. For paramedian and median placements at posterior locations, anterior tipping of the implant was found to be beneficial. For an anterior median placement, posterior tipping appeared advantageous. Age- or sex-related differences could not be observed, but variance among the subjects was generally high. Future studies are needed to identify patients at high risk of insufficient palatal bone support that may require CBCT before implant placement.

## SUPPLEMENTARY DATA

Supplementary data to this article can be found online at <https://doi.org/10.1016/j.ajodo.2018.09.019>.

## REFERENCES

1. Antoszewska-Smith J, Sarul M, Lyczek J, Konopka T, Kawala B. Effectiveness of orthodontic miniscrew implants in anchorage reinforcement during en-masse retraction: a systematic review and meta-analysis. *Am J Orthod Dentofacial Orthop* 2017;151:440-55.
2. Rizk MZ, Mohammed H, Ismael O, Beam DR. Effectiveness of en masse versus two-step retraction: a systematic review and meta-analysis. *Prog Orthod* 2018;18:41.
3. Becker K, Wilmes B, Grandjean C, Vasudavan S, Drescher D. Skeletally anchored mesialization of molars using digitized casts and two surface-matching approaches: analysis of treatment effects. *J Orofac Orthop* 2018;79:11-8.
4. Rodriguez de Guzman-Barrera J, Saez Martinez C, Boronat-Catala M, Montiel-Company JM, Paredes-Gallardo V, Gandia-Franco JL, et al. Effectiveness of interceptive treatment of class III malocclusions with skeletal anchorage: a systematic review and meta-analysis. *PLoS One* 2017;12:e0173875.
5. Kanomi R. Mini-implant for orthodontic anchorage. *J Clin Orthod* 1997;31:763-7.
6. Wilmes B, Drescher D. Application and effectiveness of the Beneslider: a device to move molars distally. *World J Orthod* 2010;11:331-40.
7. Wilmes B, Neuschulz J, Safar M, Braumann B, Drescher D. Protocols for combining the Beneslider with lingual appliances in Class II treatment. *J Clin Orthod* 2014;48:744-52.
8. Kravitz ND, Kusnoto B. Risks and complications of orthodontic miniscrews. *Am J Orthod Dentofacial Orthop* 2007;131:S43-51.
9. Bernhart T, Vollgruber A, Gahleitner A, Dortbudak O, Haas R. Alternative to the median region of the palate for placement of an orthodontic implant. *Clin Oral Implants Res* 2000;11:595-601.

10. Ryu JH, Park JH, Vu Thi Thu T, Bayome M, Kim Y, Kook YA. Palatal bone thickness compared with cone-beam computed tomography in adolescents and adults for mini-implant placement. *Am J Orthod Dentofacial Orthop* 2012;142:207-12.
11. Marquezan M, Nojima LI, Freitas AO, Baratieri C, Alves Junior M, Nojima Mda C, et al. Tomographic mapping of the hard palate and overlying mucosa. *Braz Oral Res* 2012;26:36-42.
12. Manjula WS, Murali RV, Kumar SK, Tajir F, Mahalakshmi K. Palatal bone thickness measured by palatal index method using cone-beam computed tomography in nonorthodontic patients for placement of mini-implants. *J Pharm Bioallied Sci* 2015;7:S107-10.
13. Lai RF, Zou H, Kong WD, Lin W. Applied anatomic site study of palatal anchorage implants using cone beam computed tomography. *Int J Oral Sci* 2010;2:98-104.
14. King KS, Lam EW, Faulkner MG, Heo G, Major PW. Vertical bone volume in the paramedian palate of adolescents: a computed tomography study. *Am J Orthod Dentofacial Orthop* 2007;132:783-8.
15. King KS, Lam EW, Faulkner MG, Heo G, Major PW. Predictive factors of vertical bone depth in the paramedian palate of adolescents. *Angle Orthod* 2006;76:745-51.
16. Kim HK, Moon SC, Lee SJ, Park YS. Three-dimensional biometric study of palatine rugae in children with a mixed-model analysis: a 9-year longitudinal study. *Am J Orthod Dentofacial Orthop* 2012;141:590-7.
17. Kang S, Lee SJ, Ahn SJ, Heo MS, Kim TW. Bone thickness of the palate for orthodontic mini-implant anchorage in adults. *Am J Orthod Dentofacial Orthop* 2007;131:574-81.
18. Jung BA, Wehrbein H, Heuser L, Kunkel M. Vertical palatal bone dimensions on lateral cephalometry and cone-beam computed tomography: implications for palatal implant placement. *Clin Oral Implants Res* 2011;22:664-8.
19. Hourfar J, Ludwig B, Bister D, Braun A, Kanavakis G. The most distal palatal ruga for placement of orthodontic mini-implants. *Eur J Orthod* 2015;37:373-8.
20. Hourfar J, Kanavakis G, Bister D, Schatzle M, Awad L, Nienkemper M, et al. Three dimensional anatomical exploration of the anterior hard palate at the level of the third ruga for the placement of mini-implants—a cone-beam CT study. *Eur J Orthod* 2015;37:589-95.
21. Gracco A, Lombardo L, Cozzani M, Siciliani G. Quantitative cone-beam computed tomography evaluation of palatal bone thickness for orthodontic miniscrew placement. *Am J Orthod Dentofacial Orthop* 2008;134:361-9.
22. de Rezende Barbosa GL, Ramirez-Sotelo LR, Tavora DM, Almeida SM. Comparison of median and paramedian regions for planning palatal mini-implants: a study in vivo using cone beam computed tomography. *Int J Oral Maxillofac Surg* 2014;43:1265-8.
23. Baumgaertel S. Cortical bone thickness and bone depth of the posterior palatal alveolar process for mini-implant insertion in adults. *Am J Orthod Dentofacial Orthop* 2011;140:806-11.
24. Baumgaertel S. Quantitative investigation of palatal bone depth and cortical bone thickness for mini-implant placement in adults. *Am J Orthod Dentofacial Orthop* 2009;136:104-8.
25. Ludwig B, Glasl B, Bowman SJ, Wilmes B, Kinzinger GS, Lisson JA. Anatomical guidelines for miniscrew insertion: palatal sites. *J Clin Orthod* 2011;45:433-41.
26. Wilmes B, Drescher D. A miniscrew system with interchangeable abutments. *J Clin Orthod* 2008;42:574-80.
27. Wilmes B, Ludwig B, Vasudavan S, Nienkemper M, Drescher D. The T-zone: median vs paramedian insertion of palatal mini-implants. *J Clin Orthod* 2016;50:543-51.
28. Bernhart T, Freudenthaler J, Dortbudak O, Bantleon HP, Watzek G. Short epithetic implants for orthodontic anchorage in the paramedian region of the palate. A clinical study. *Clin Oral Implants Res* 2001;12:624-31.
29. R-Core-Team. R. A language and environment for statistical computing. Vienna, Austria: R Foundation for Statistical Computing; 2016. Available at: <https://www.R-project.org>.
30. Gahleitner A, Podesser B, Schick S, Watzek G, Imhof H. Dental CT and orthodontic implants: imaging technique and assessment of available bone volume in the hard palate. *Eur J Radiol* 2004;51:257-62.
31. Kawa D, Kunkel M, Heuser L, Jung BA. What is the best position for palatal implants? A CBCT study on bone volume in the growing maxilla. *Clin Oral Investig* 2017;21:541-9.
32. Wilmes B, Su YY, Drescher D. Insertion angle impact on primary stability of orthodontic mini-implants. *Angle Orthod* 2008;78:1065-70.
33. Holm M, Jost-Brinkmann PG, Mah J, Bumann A. Bone thickness of the anterior palate for orthodontic miniscrews. *Angle Orthod* 2016;86:826-31.
34. Sumer AP, Caliskan A, Uzun C, Karoz TB, Sumer M, Cankaya S. The evaluation of palatal bone thickness for implant insertion with cone beam computed tomography. *Int J Oral Maxillofac Surg* 2016;45:216-20.
35. Wehrbein H. Bone quality in the midpalate for temporary anchorage devices. *Clin Oral Implants Res* 2009;20:45-9.
36. Baxter-Jones AD, Faulkner RA, Forwood MR, Mirwald RL, Bailey DA. Bone mineral accrual from 8 to 30 years of age: an estimation of peak bone mass. *J Bone Miner Res* 2011;26:1729-39.
37. Stockmann P, Schlegel KA, Srour S, Neukam FW, Fenner M, Felszeghy E. Which region of the median palate is a suitable location of temporary orthodontic anchorage devices? A histomorphometric study on human cadavers aged 15-20 years. *Clin Oral Implants Res* 2009;20:306-12.
38. Milovanovic P, Adamu U, Simon MJ, Rolvien T, Djuric M, Amling M, et al. Age- and sex-specific bone structure patterns portend bone fragility in radii and tibiae in relation to osteodensitometry: a high-resolution peripheral quantitative computed tomography study in 385 individuals. *J Gerontol A Biol Sci Med Sci* 2015;70:1269-75.
39. Macdonald HM, Nishiyama KK, Kang J, Hanley DA, Boyd SK. Age-related patterns of trabecular and cortical bone loss differ between sexes and skeletal sites: a population-based HR-pQCT study. *J Bone Miner Res* 2011;26:50-62.
40. de Rezende Barbosa GL, Ramirez-Sotelo LR, Tavora Dde M, de Almeida SM. Vertical measurements for planning palatal mini-implants in lateral radiography and cone beam computed tomography. *Implant Dent* 2014;23:588-92.
41. Pauwels R, Jacobs R, Singer SR, Mupparapu M. CBCT-based bone quality assessment: are Hounsfield units applicable? *Dentomaxillofac Radiol* 2015;44: 20140238.
42. Pauwels R, Nackaerts O, Bellaiche N, Stamatakis H, Tsiklakis K, Walker A, et al. Variability of dental cone beam CT grey values for density estimations. *Br J Radiol* 2013;86: 20120135.
43. Winsauer H, Vlachojannis C, Bumann A, Vlachojannis J, Chrubasik S. Paramedian vertical palatal bone height for mini-implant insertion: a systematic review. *Eur J Orthod* 2014;36:541-9.
44. Wehrbein H. Anatomic site evaluation of the palatal bone for temporary orthodontic anchorage devices. *Clin Oral Implants Res* 2008;19:653-6.